Journal of
Computational and Theoretical Nanoscience
Vol. 6, 106–111, 2009

Numerical Study of Optical Properties of $Ag/SiO_2/Ag$ Sandwich Nanobowties

Lanying Yang, Chunlei Du, and Xiangang Luo*

State Key Laboratory of Optical Technologies for Microfabrication, Institute of Optics and Electronics, Chinese Academy of Science, P.O. Box 350, Chengdu 610209, China

A composite nanobowtie with $Ag/SiO_2/Ag$ sandwich structure is presented and its optical properties especially the Plasmon property are studied using the discrete dipole approximation (DDA) method in this paper. Our results show that this structure has simply-tunable surface Plasmon resonance (SPR) wavelengths and more "hotter spots" provided by the sandwich structure, as well as the remarkable enhancement of the localized *E*-field provided by the bowtie structure. The transverse and longitudinal Plasmon coupling mechanism is employed to explain tunable SPR and strong *E*-field enhancement respectively. The sandwich nanobowtie possesses the qualities of simply-tunable SPR and great *E*-field enhancement, thereby holding a great potential in applications such as surface-enhanced Raman scattering (SERS).

Keywords: Sandwich, Bowtie, DDA, SPR.

1. INTRODUCTION

Metallic nanoparticles with various shape and structure, including nanotriangles, nanoprisms, nanorings, nanopin and nanophotonic crescents, have been explored and developed to be nanoplasmonic resonators in recent years.[1–10] These nanoplasmonic resonators exhibit local-field enhancement and have been proven to be very unique for biomolecular labeling and detection, subwavelength lithography and nonlinear optical devices.[11–15] Especially the bowtie structure which is configured with two opposing tip-to-tip nanotriangles and separated by a nanogap, once exhibits remarkably large local *E*-field enhancement and strong scattering and has been widely studied in many fields such as optical antenna, optical waveguide, and SERS.[16–19] However, the Plasmon frequencies of these nanoplasmonic resonators are usually tuned by the particle size and shape in recent years because the plasmonic properties of metallic nanoparticles depend on their size, shape, and dielectric environment.[20–22] In fact, both simply-tunable SPR and large *E*-field enhancement are two key factors for nanoplasmonic resonators to improve their performance and extend their afore-mentioned applications especial in the SERS field.

In this paper, a special composite nanostructure i.e., $Ag/SiO_2/Ag$ sandwich nanobowtie, which has an $Ag/SiO_2/Ag$ sandwich structure vertically and a bowtie structure horizontally, is presented. The optical properties especially the plasmonic properties of the sandwich nanobowtie are explored. Our results show that the structure of the sandwich bowtie combines the virtue of simply-tunable SPR wavelength provided by the sandwich structure and the virtue of large enhancement of *E*-fields from the bowtie structure, and therefore holds unique optical properties for application in SERS. To our knowledge, this is the first report regarding optical properties of the nanobowtie with sandwich structure.

2. SIMULATION METHOD AND SETUP

The sandwich bowtie investigated is composed of two silver bowties and one SiO_2 layer between the two metal layers as shown in Figure 1. Both the Ag and the SiO_2 triangular prisms have the same side length of 60 nm and different thickness. The former has a fixed thickness of 12 nm and the latter has a varying thickness. Both the *Y* axis and *Z* axis are defined in the triangle plane, while the *X* axis is along the thickness of the structure. In addition, parameter *h* is defined as the thickness of the dielectric (i.e., SiO_2) layer.

All numerical calculations are performed on the basis of the discrete dipole approximation (DDA) method, which is popular and flexible for calculating optical properties of nanoparticles with arbitrary shape.[23–27] In the DDA approximation, the nanobowtie is represented by an array of *N* dipoles which locate on a cubic lattice and have

*Author to whom correspondence should be addressed.

1546-1955/2009/6/106/006 doi:10.1166/jctn.2009.1014

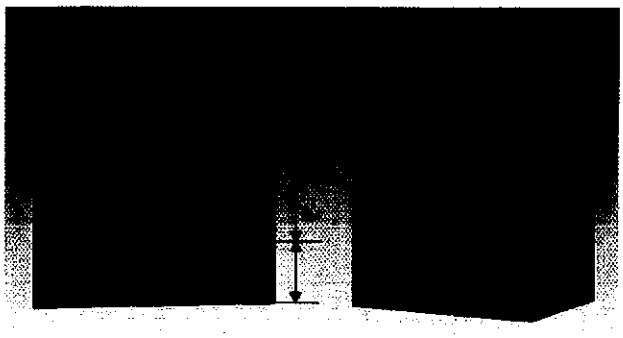

Fig. 1. Schematic drawing of the sandwich Ag/SiO_2/Ag nanobowtie. Here the top and the bottom silver layers have fixed thickness of 12 nm and the middle dielectric layer has varying thickness.

polarizability ∂_i $(i = 1 \ldots N)$.[27] The dipole moment of the element located at r_i is $P_i = \partial_i E_{\text{loc},i}$, where the local field $E_{\text{loc},i}$ is a sum of the incident field $E_{\text{inc},i}$ and the field radiated by all the other dipoles in the system $E_{\text{dip},i}$,[22,25] i.e.,

$$E_{\text{loc},i} = E_{\text{inc},i} + \sum_{k \neq i} E_{\text{dip},i} \tag{1}$$

Substituting the expression for the dipole moment, representing the radiation from a dipole $E_{\text{dip},k}$ as $E_{\text{dip},k} = A_{jk}P_k$, and rearranging yields,

$$\partial^{-1} P_i - \sum_{j \neq k} A_{jk} P_k = E_{\text{inc},i} \tag{2}$$

using the well-known expression for radiation of a dipole located at position r_k evaluated at point r_i,[22,25]

$$A_{jk}P_k = \frac{\exp[ikr_{jk}]}{r_{jk}^3} \times \left\{ k^2 r_{jk} \times (r_{jk} \times P_k) + \left(\frac{1}{r_{jk}^2} - \frac{ik}{r_{jk}} \right) \times [r_{jk}^2 P_k - 3r_{jk}(r_{jk} \cdot P_k)] \right\} \tag{3}$$

Where k is the wave vector of the incident wave, r_{jk} is a unit vector pointing from r_k to r_i, and $r_{jk} = |r_j - r_k|$. Defining $A_{ii} = \partial_i^{-1}$, the Eqs. (2) and (3) can be simplified and then written as a single matrix equation as following:[22,25]

$$\tilde{A} \cdot \tilde{P} = \tilde{E}_{\text{inc}} \tag{4}$$

Where $\tilde{A}$ is a $3_N \times 3_N$ matrix which describes the interactions between dipoles, $\tilde{E}_{\text{inc}}$ is a $3_N \times 1$ vector, and $\tilde{P}$ is a $3_N \times 1$ vector of unknown dipole moments. Once Eq. (4) has been solved for the unknown polarization P_i, the extinction C_{ext}, absorption C_{abs} and scattering C_{sca} cross sections can be evaluated as following:[22,25]

$$C_{\text{ext}} = \frac{4\pi k}{|E_0|^2} \sum_{i=1}^{N} Im(E_{\text{loc},i}^* \cdot P_i) \tag{5}$$

$$C_{\text{abs}} = \frac{4\pi k}{|E_0|^2} \sum_{i=1}^{N} \left\{ Im[P_i \cdot (\partial_i^{-1})^* P_i^*] - \frac{2}{3} k^3 |P_i|^2 \right\} \tag{6}$$

$$C_{\text{sca}} = C_{\text{ext}} - C_{\text{abs}} \tag{7}$$

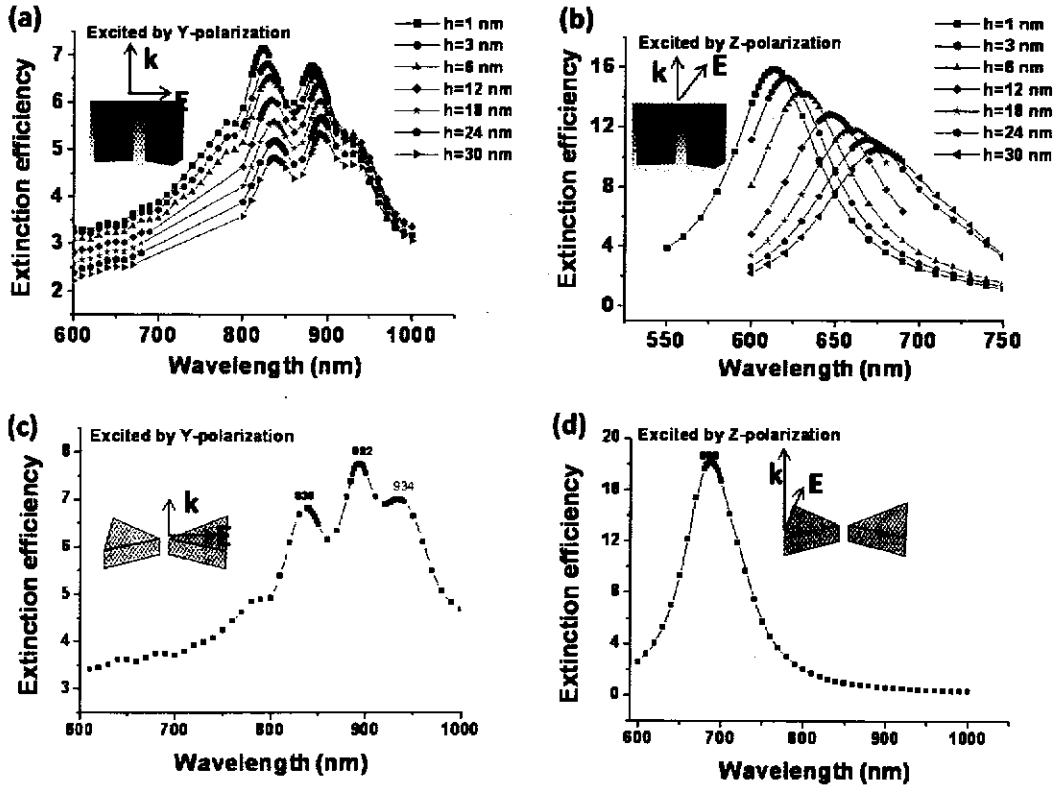

Fig. 2. Extinction spectra of the sandwich nanobowtie with the thickness of SiO_2 layer varying from 1 nm to 30 nm, excited by (a) Y-polarization and (b) Z-polarization, extinction spectra of the non-sandwich nanobowtie, excited by (c) Y-polarization and (d) Z-polarization.

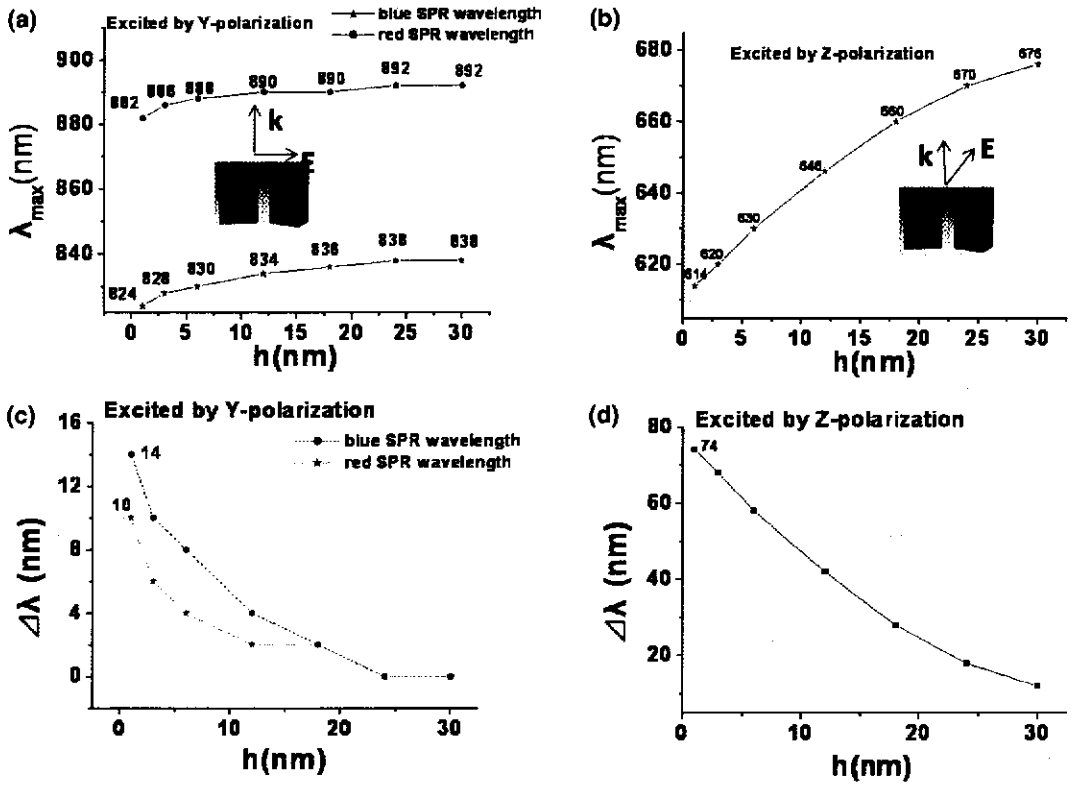

Fig. 3. (a–b) The SPR wavelength of the sandwich nanobowtie as a function of the thickness of SiO_2 layer, and (c–d) the SPR wavelength shift of the sandwich nanobowtie relative to that of the single-layer bowtie as a function of the thickness of SiO_2 layer, excited by *Y*-polarization (a, c) and *Z*-polarization (b, d).

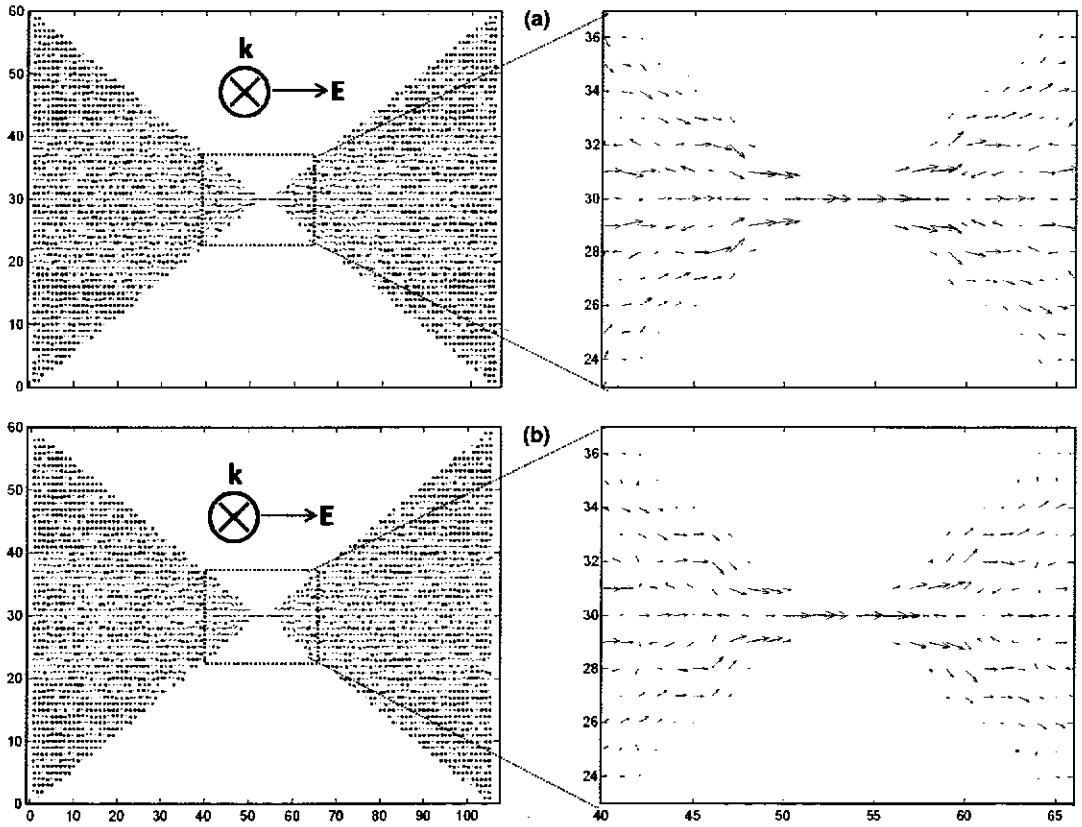

Fig. 4. Polarization vectors for dipole resonance at 828 nm (a) and 886 nm (b) of the sandwich bowtie with $h = 3$ nm.

So the extinction Q_{ext}, absorption Q_{abs} and scattering Q_{sca} efficiency factor can also be evaluated, i.e.,

$$Q_{ext} = \frac{C_{ext}}{\pi \partial_{eff}^2} \quad (8)$$

$$Q_{abs} = \frac{C_{abs}}{\pi \partial_{eff}^2} \quad (9)$$

$$Q_{sca} = \frac{C_{sca}}{\pi \partial_{eff}^2} \quad (10)$$

Where ∂_{eff} is the effective radius which characterized the size of the nanobowtie. If let V be the nanobowtie's volume, then ∂_{eff} is defined as following:

$$\partial_{eff} = \left(\frac{3V}{4\pi}\right)^{1/3} \quad (11)$$

In all DDA calculations, the glass substrate is taken into account by embedding the particle in a homogeneous medium with the averaged refractive index of air and glass,[5] the silver dielectric constant is taken from Palik[28] but smoothed as described by Jensen,[29] the permittivity of SiO_2 is set to be 2.13, and a cubic grid with a spacing of 1 nm is used.

3. RESULTS AND DISCUSSION

As can be seen in Figures 2(a and b), there are some differences between the Y-polarized and Z-polarized extinction spectra for sandwich bowties. There are two obvious SPR peaks in the extinction spectra (we call them blue and red SPR wavelength, respectively) for Y-polarization at different dielectric thickness but a single SPR peak in Z-polarized extinction spectra. All the SPR peaks for Y-polarization and Z-polarization blue shift relative to those of the single-layer bowtie which locate at 838, 892, and 688 nm respectively (see Figs. 2(c–d)). But with the increase of the thickness of the SiO_2 layer from 1 to 30 nm the blue and red SPR wavelength for Y-polarization red shift from 882 to 892 nm and from 824 to 838 nm respectively, as can be seen in Figure 3(a). The Z-polarized SPR peak has the same trend, which red shifts from 614 to 676 nm with the dielectric thickness changing from 1 to 30 nm (see Fig. 3(b)). Considering the SPR blue-shift relative to that of single-layer bowtie in detail in Figures 3(c–d), there is an obvious decrease in SPR blue-shift with the dielectric thickness increasing for both Y- and Z-polarization. The shifts of the Y-polarized SPR peaks are up to 14 and 10 nm for the blue and red SPR peak respectively, while that of the Z-polarized SPR peak

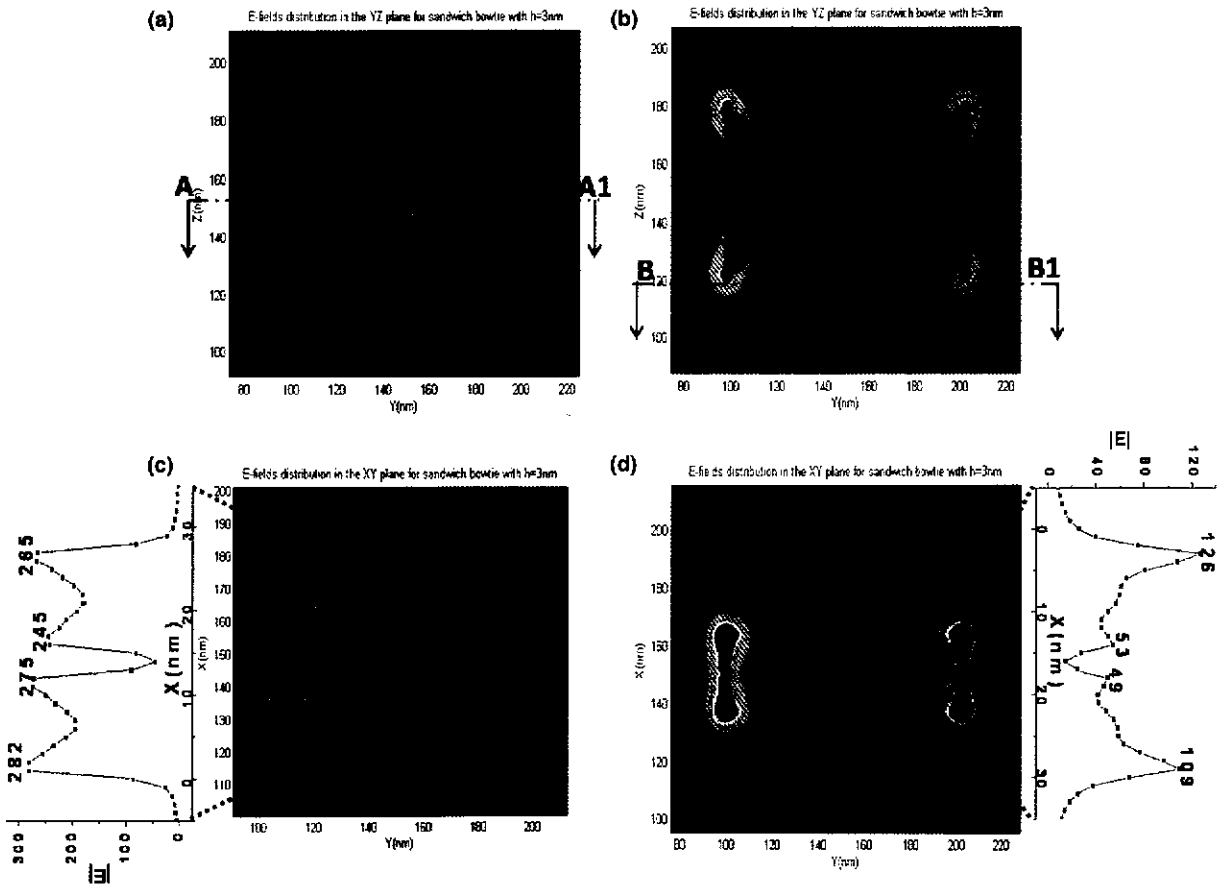

Fig. 5. Normalized E-fields distribution of sandwich bowtie in the YZ plane (a–b) and the corresponding section plane along the section line AA1 and BB1, for Y-polarization (a, c) and Z-polarization (b, d), with the thickness of SiO_2 layer of 3 nm.

can be up to 74 nm when the dielectric layer is only 1 nm thick. It clearly shows that the blue peak exhibits a slight more dependence on the thickness of the dielectric layer than the red peak for Y-polarized SPR, while the Z-polarized SPR peak exhibits a few more dependence than the both SPR peaks excited by Y-polarization. It's obvious that the SPR frequency of the sandwich bowtie can be easily-tuned by varying the thickness of SiO_2 layer.

The above-mentioned behavior that SPR peaks of the sandwich bowtie blue shift relative to that of single-layer bowtie can be explained by the transverse Plasmon coupling between the top and the bottom metal layer. Considering the sandwich bowtie as two silver bowties coupled vertically, then the excitation electric field with Y or Z polarization is perpendicular to the bowtie center–center axis, accordingly there is a Plasmon coupling in transverse mode. Previous study shows that the transverse Plasmon coupling lead to the enhancement of the repulsive force for the surface charges, thereby the particle Plasmon energy increases and causes a blue-shift of SPR wavelength.[4, 31] Therefore with the increase of the dielectric layer thickness, the Plasmon coupling strength decreases and the SPR wavelength is closer to that of the single-layer bowtie.

To investigate the two SPR peaks for Y-polarization are from the dipole or the quadrupole resonance, the polarization vectors of sandwich bowtie with $h = 3$ nm at both SPR wavelengths are also plotted in Figure 4. Here only the imaginary component is plotted because it contains the crucial information of the particle's extinction behavior.[30] The polarization vectors at blue (828 nm) and red (886 nm) SPR peak are aligned along the Y axis with the largest induced polarization occurring at the opposite tips in the gap. This behavior appears analogous to the dipole resonance of bowtie described in previous literature,[27] so we conjecture the two SPR are both from dipole resonance.

To consider the E-field distribution around the sandwich bowtie, the amplitude distributions of the total E-field outside of the particle in the YZ and XY plane are simulated. As can be seen from Figures 5 and 6, most of "hot spots" of sandwich bowties are still at the same locations with those of the single-layer bowtie for both Y- and Z-polarization, i.e., the "hot spots" mainly locate in the middle of the gap (see Fig. 5(a)) and near the corners of the triangle (see Fig. 5(b)) for Y- and Z-polarization respectively. The averaged amplitude enhancement over the "hotter spots" of the metal layers is over 200 and 60 for Y- and Z-polarization respectively, furthermore the corresponding maximum enhancement of amplitude is up to 282 and 126 (see Figs. 5(c–d)), exhibiting great E-field amplification. This strong E-field enhancement of sandwich bowtie is like that of the single-layer bowtie in Figure 6, therefore it should result from the near-field

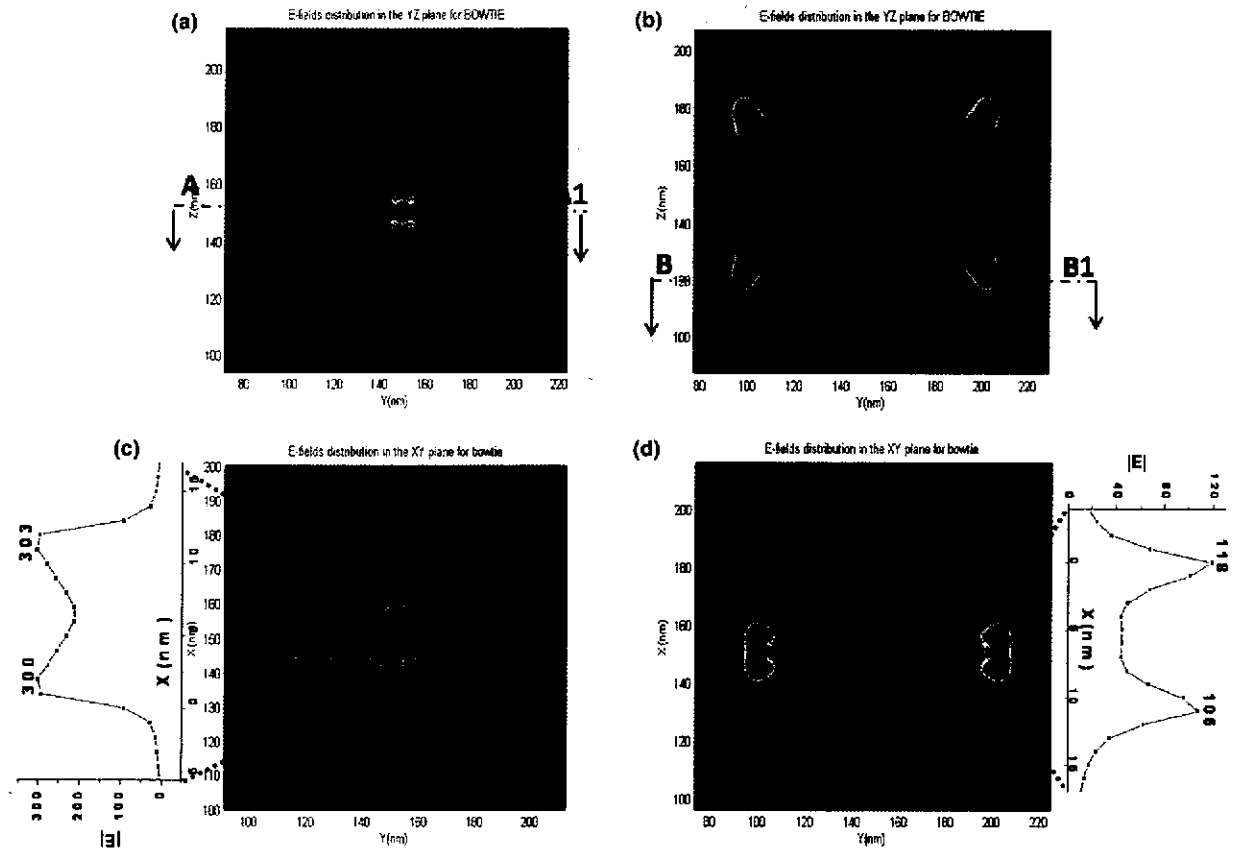

Fig. 6. Normalized E-fields distribution of bowtie in the YZ plane (a–b) and the corresponding section plane along the section line AA1 and BB1, for Y-polarization (a, c) and Z-polarization (b, d).

longitudinal Plasmon coupling of two horizontally-facing triangles in the bowtie structure as stated in previous literatures.[2,4] Moreover, the sandwich bowtie has more "hot spots" than the single-layer bowtie resulting from the increased interfaces. There are four distinctive "hotter spots" in the gap of the sandwich bowtie in Figures 5(c–d) and only two distinctive "hotter spots" in the gap of the non-sandwich bowtie in Figure 6(c–d). So it's inferred that there will be more "hotter spots" if multilayered Ag/SiO_2 is inserted into the sandwich bowtie. The remarkable E-field enhancement and more "hotter spots"demonstrated by the sandwich nanobowtie are very important for SERS.

4. SUMMARY

In summary, the optical properties especially plasmonic properties of the sandwich nanobowtie are investigated. The extinction spectra with various dielectric thickness are simulated, showing a remarkable blue-shift relative to single-layer bowtie for both Y- and Z-polarization. Moreover, the blue-shift decreases with the dielectric thickness increasing and the Z-polarized SPR shows more dependence on the SiO_2 thickness. These behaviors can be explained by the near-field Plasmon coupling in transverse mode. The E-field amplitude distributions outside the nanobowtie are also investigated both in the XY and YZ plane, demonstrating strong averaged amplitude enhancement of the electric field over "hotter spots." In addition, the sandwich bowtie has more "hot spots" than the single-layer bowtie because of increased interfaces. It can be conclude that the sandwich nanobowtie has simply-tunable PR and many "hotter spots" provided by the sandwich structure and large enhanced E-fields provided by the bowtie structure, thereby holding a great potential in applications such as surface-enhanced Raman scattering.

Acknowledgments: The authors would like to thank the financial support from 973 Program (Grant No. 2006CB302900) and the Chinese Nature Science Grant 60678035 and 60507014. The authors also thank Hongtao Gao, Yanzhong Chen, Ting Xu, Haofei Shi, Wei Wang, and Xiong Li for their kind contribution to this work.

References

1. S. Wang, D. F. P. Pile, C. Sun, and X. Zhang, *Nano. Lett.* 7, 1076 (**2007**).
2. K. H. Su, Q. H. Wei, X. Zhang, J. J. Mock, D. R. Smith, and S. Schultz, *Nano. Lett.* 3, 1087 (**2003**).
3. Y. Lu, G. L. Liu, J. Kim, Y. X. Mejia, and L. P. Lee, *Nano Lett.* 5, 119 (**2005**).
4. K. H. Su, Q. H. Wei, and X. Zhang, *Appl. Phys. Lett.* 88, 063118 (**2006**).
5. K.-H. Su, S. Durant, J. M. Steele, Y. Xiong, C. Sun, and X. Zhang, *J. Phys. Chem. B* 110, 3964 (**2006**).
6. Y. Fu, W. Zhou, L. E. N. Lennie, C. Du, and X. Luo, *Appl. Phys. Lett.* 91, 061124 (**2007**).
7. J. H. Amanda, L. H. Christy, D. M. Adam, G. C. Schatz, R. P. Van Duyne, and S. Zou, *MRS Bull.* 30, 368 (**2005**).
8. J. S. Leif, R. Jin, C. A. Mirkin, G. C. Schatz, and R. P. Van Duyne, *Nano. Lett.* 6, 2060 (**2006**).
9. S. Link and M. A. El-Sayed, *J. Phys. Chem. B* 103, 8410 (**1999**).
10. T. K. Sau and C. J. Murphy, *Langmuir* 20, 6414 (**2004**).
11. S. Schultz, D. R. Smith, J. J. Mock, and D. A. Schultz, *Proc. Natl. Acad. Sci. USA* 97, 996 (**2000**).
12. A. J. Haes and R. P. Van Duyne, *J. Am. Chem. Soc.* 124, 10596 (**2002**).
13. S. O. Obare, R. E. Hollowell, and C. J. Murphy, *Langmuir* 18, 10407 (**2002**).
14. C. E. H. Berger, T. A. M. Beumer, R. P. H. Kooyman, and J. Greve, *Anal. Chem.* 70, 703 (**1998**).
15. J. Aizpurua, P. Hanarp, D. S. Sutherland, M. Kall, G. W. Bryant, and F. J. Garcia de Abajo, *Phys. Rev. Lett.* 90, 057401 (**2003**).
16. A. Sundaramurthy, P. J. Schuck, N. R. Conley, D. P. Fromm, G. S. Kino, and W. E. Moerner, *Nano. Lett.* 6, 355 (**2006**).
17. D. P. Fromm, A. Sundaramurthy, A. Kinkhabwala, and P. J. Schuck, G. S. Kino, and W. E. Moerner, *J. Chem. Phys.* 124, 061101 (**2006**).
18. N. F. Javad, H.-J. Eisler, D. W. Pohl, M. Pavius, P. Fluckiger, P. Gasser, and B. Hecht, *Nanotech.* 18, 125506 (**2007**).
19. A. Sundaramurthy, K. B. Crozier, and G. S. Kino, *Phys. Rev. B* 72, 165409 (**2005**).
20. E. Hao and G. C. Schatz, *J. Chem. Phys.* 120, 357 (**2004**).
21. Z. Y. Zhang and Y. P. Zhao, *Appl. Phys. Lett.* 89, 023110 (**2006**).
22. K. L. Kelly, E. Coronado, L. L. Zhao, and G. C. Schatz, *J. Phys. Chem. B* 107, 668 (**2003**).
23. B. T. Draine and P. J. Flatau, *J. Opt. Soc. Am. A* 11, 1491 (**1994**).
24. K. Muinonen and E. Zubko, *J. Quanti. Spec. & Radi. Trans.* 100, 288 (**2006**).
25. N. Felidj, J. Aubard, and G. Levi, *J. Chem. Phys.* 111, 1195 (**1999**).
26. T. R. Jensen, G. C. Schatz, and R. P. Van Duyne, *J. Phys. Chem. B* 103, 2394 (**1999**).
27. B. T. Draine and P. J. Flatau, *J. Opt. Soc. Am.* 11, 1491 (**1973**); "User's Guide to the Discrete Dipole Approximation Code DSCAT. 6.0," 2003, http://arxiv.org/abs/astro-ph/0300969, Accessed 2008.
28. E. D. Palik, Handbook of Optical Constants of Solids, Academic, New York (**1985**).
29. T. Jensen, K. L. Kelly, A. Lazarides, and G. C. Schatz, *J. Cluster Sci.* 10, 295 (**1999**).
30. W. Rechberger, A. Hohenau, A. Leitner, J. R. Krenn, B. Lamprecht, and F. R. Ausenegg, *Opt. Commun.* 220, 137 (**2003**).
31. K. L. Kelly, Classical Electrodynamics of Surface Enhancing Nanoparticles, ProQuest Information and Learning Company, Ann Arbor, USA (**2002**).

Received: 20 May 2008. Accepted: 26 June 2008.